JACS
JOURNAL OF THE AMERICAN CHEMICAL SOCIETY

COMMUNICATION

pubs.acs.org/JACS

Phosphorescent Sensor for Robust Quantification of Copper(II) Ion

Youngmin You,[*,†,‡] Yejee Han,[‡] Yong-Min Lee,[‡] Soo Young Park,[§] Wonwoo Nam,[*,‡] and Stephen J. Lippard[*,†]

[†]Department of Chemistry, Massachusetts Institute of Technology, Cambridge, Massachusetts 02139, United States

[‡]Department of Bioinspired Science, Ewha Womans University, Seoul 120-750, Korea

[§]Department of Materials Science and Engineering, Seoul National University, Seoul 151-744, Korea

Supporting Information

ABSTRACT: A phosphorescent sensor based on a multichromophoric iridium(III) complex was synthesized and characterized. The construct exhibits concomitant changes in its phosphorescence intensity ratio and phosphorescence lifetime in response to copper(II) ion. The sensor, which is reversible and selective, is able to quantify copper(II) ions in aqueous media, and it detects intracellular copper ratiometrically.

The facile redox chemistry and strong ligand binding properties of the copper ion are key factors that underlie its essential biological functions that include energy generation, dioxygen transport and activation, and signal transduction. Understanding the biological and environmental roles of copper(II) ion requires robust and versatile methods for quantification.[1−3] This task is challenging because fast electron and energy transfer involving paramagnetic copper centers results in strong fluorescence quenching for most luminescent sensors.[4] The goal has been to devise "turn-on" fluorescent sensors for copper(II), selected strategies for which include opening of a spirolactam,[5−7] suppression of non-emissive electronic transitions of a conjugated imine,[8,9] excimer formation,[10,11] photolysis of a copper(II) ionophore,[12] and a displacement assay in a catalytic system for generating a fluorescent indicator.[13] These turn-on signals are, however, insufficient for quantification. An alternative approach involves sensors that display a change in the ratio of multiple emission bands, providing quantification as a significant advantage.[14−16] Few ratiometric fluorescent copper sensors are available,[17−19] however, and those that do exist suffer from limited versatility, including instability in a polar medium, long response time, and irreversibility.

A promising approach for ratiometric Cu(II) sensing is a platform that provides dual-wavelength emission following single-wavelength excitation. This effect is in apparent violation of Kasha's rule, which dictates single emission from the lowest excited state.[20] The known exceptions involve phosphorescent transition metal complexes, such as heteroleptic Ru(II)[21−24] and Re(I)[25−28] complexes, in which limited internal conversion between two metal-to-ligand charge-transfer (MLCT) transition states accounts for the dual emission. We previously identified multichromophoric centers of phosphorescent heteroleptic Ir(III) complexes. Here, internal conversion depends strongly on ligand structure,[29−31] and dual emission occurs for both cationic[32] and charge-neutral[33] Ir(III) complexes. Encouraged by these observations, we sought to develop a phosphorescence ratiometric sensor based on an Ir(III) construct. Phosphorescent Ir(III) complexes are appealing platforms because they exhibit highly efficient room-temperature phosphorescence as a consequence of efficient intersystem crossing provided by Ir.[34−37] In addition, their long-lifetime emission (typically several microseconds) is unaffected by short-lived background noise such as fluorescence and scattered light. As for ratiometric detection, changes in luminescence lifetime are determined solely by the concentration of the analyte of interest.[38−40] A combination of phosphorescence ratiometric signals and phosphorescence lifetime therefore offers a powerful tool for quantification of copper(II) ion.

Scheme 1. Synthesis and Structure of the Copper(II) Sensor ZIr2

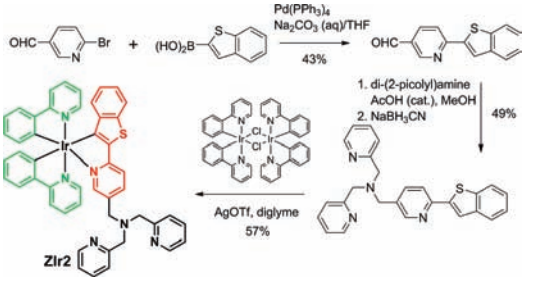

In the present work we prepared a ratiometric copper(II) sensor (ZIr2) based on a multichromophoric Ir(III) complex having one 2-(2′-benzo[*b*]thienyl)pyridine (btp) and two cyclometalating 2-phenylpyridine (ppy) ligands.[33] A di(2-picolyl)amine (DPA) copper ion receptor was tethered to the btp ligand by a methylene linker. Dual phosphorescence, green from the ppy ligands and red from the btp ligand, occurs in the absence of copper(II) ion, but copper complexation to the DPA moiety preferentially quenches red emission from the adjacent btp ligand (see photo in Supporting Information (SI), Figure S1). Thus, a ratiometric signal is obtained by dual emission, with green and red bands corresponding to the reference and probe signals, respectively. In addition, a decrease in phosphorescence lifetime of the red emission can be used to validate the copper-induced change.

The iridium(III) complex (ZIr2) was prepared in four steps with an overall yield of 9% (Scheme 1) and fully characterized by a variety of spectroscopic methods (SI). A reference Ir(III)

Received: May 31, 2011
Published: July 12, 2011

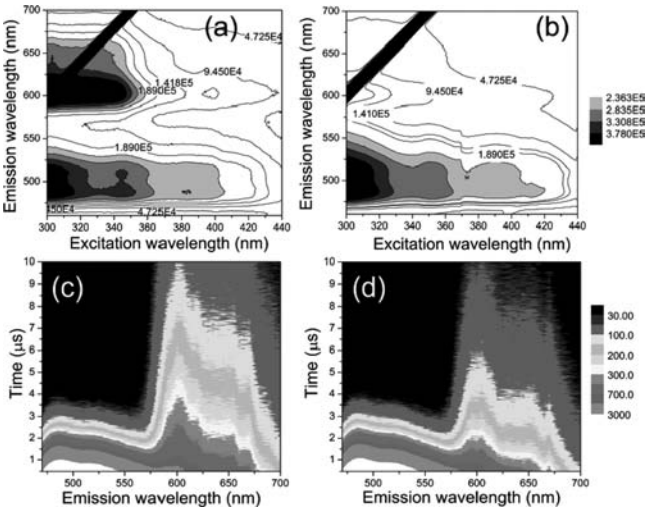

Figure 1. Steady-state phosphorescence spectrum of ZIr2 in the absence (a) and presence (b) of $CuCl_2$. Time-resolved phosphorescence spectrum of ZIr2 in the absence (c) and presence (d) of $CuCl_2$ (λ_{ex} = 342 nm). Conditions: 10 μM ZIr2 for steady-state spectra and 20 μM ZIr2 for time-resolved spectra in pH 7.0 buffer (25 mM PIPES containing <2 vol % of DMSO). Black diagonal lines in (a) and (b) are harmonics of the excitation beam.

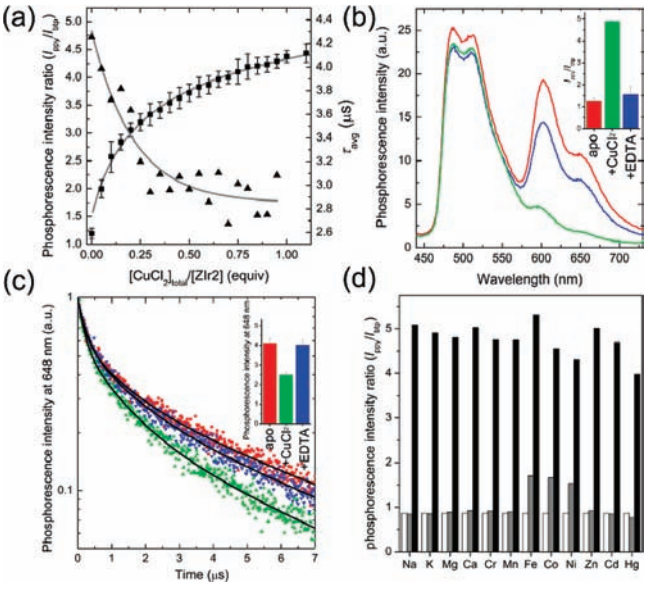

Figure 2. (a) Phosphorescence titration (■, phosphorescence intensity ratio (I_{ppy}/I_{btp}); ▲, average phosphorescence lifetime, τ_{avg}) of ZIr2 with the addition of $CuCl_2$. See Figures S3 and S5 in Supporting Information for the raw data. (b) Reversible change in phosphorescence spectrum of ZIr2 in response to $CuCl_2$ (red line, Cu(II)-free state; green line, in the presence of $CuCl_2$ (1 equiv); blue line, after subsequent addition of Na_2EDTA (100 equiv) to the mixture). The inset depicts the corresponding change in phosphorescence intensity ratio of green (470−570 nm) vs red (580−700 nm) bands. (c) Reversible change in the phosphorescence decay trace of ZIr2 in response to $CuCl_2$ (red symbols, Cu(II)-free state; green symbols, in the presence of $CuCl_2$ (1 equiv); blue symbols, after subsequent addition of Na_2EDTA (200 equiv) to the mixture). Black solid lines are fits based on a triple-exponential decay model. The inset depicts the corresponding change in the average phosphorescence lifetime. (d) Cu(II) ion selectivity of ZIr2 (white bar, metal-free state; gray bar, in the presence of metal salt (100 equiv for Na^+, Mg^{2+}, Ca^{2+}; 10 equiv for Zn^{2+}; 1 equiv for others); black bar, after subsequent addition of $CuCl_2$ (1 equiv)). Conditions: 10 μM ZIr2 for steady-state measurements and 20 μM ZIr2 for time-resolved measurements in pH 7.0 buffer (25 mM PIPES containing <2 vol % of DMSO).

complex without the DPA appendage was also prepared for comparison. The absorption (SI, Figure S2) and phosphorescence spectral behavior of ZIr2 was characterized in pH 7.0 buffer (25 mM PIPES containing <2 vol % of DMSO, air-equilibrated) at 25 °C. The phosphorescence quantum yield of an air-equilibrated buffer of ZIr2 was determined to be 3.0% relative to fluorescein as a standard. The steady-state phosphorescence spectra are characterized by an apparent dual emission in the green (470−570 nm, I_{ppy}) and red (580−700 nm, I_{btp}) regions emanating from the ppy and btp ligands, respectively (Figure 1a). Addition of $CuCl_2$ (1 equiv) to the ZIr2 solution predominantly quenched the red emission, effecting a change in the ratio of green to red phosphorescence emission intensity (Figure 1b and SI, Figure S3). The increase in phosphorescence intensity ratio (I_{ppy}/I_{btp}) was ca. 4-fold.

A time-resolved emission spectrum (TRES) of the ZIr2 solution was acquired with excitation at 342 nm (Figure 1c), revealing a short-lived green (I_{ppy}) and a relatively long-lived red (I_{btp}) emission that decays more rapidly in the presence of $CuCl_2$ (Figure 1d). The dual-emission decay traces were monitored at 486 and 648 nm, corresponding to the green and red phosphorescence, respectively. The phosphorescence trace at 486 nm was fit to a single-exponential decay with a lifetime of 0.53 μs that was unaltered upon addition of $CuCl_2$ (SI, Figure S4). In contrast, the 648 nm emission lifetime decreased significantly in the presence of copper(II) ions (SI, Figure S5). The best fits for the 648 nm trace were obtained when multiexponential decay models were applied, which most likely reflects reversible or partial internal conversion from and to the green-phosphorescent ppy ligands. This result is similar to that obtained for dual-emissive Ru(II) complexes.[24] A photophysical scheme that identifies the btp ligand as being responsible for the red phosphorescence emission was derived from quantum chemical calculations based on time-dependent density functional theory (TD-DFT, B3LYP/6-31G**: LANL2DZ; see SI, Table S1). Selective quenching of the red phosphorescence arises from the proximity of the btp ligand to the paramagnetic copper(II) center. The notable decrease in phosphorescence lifetime of ZIr2 is ascribed to facile energy or electron transfer. We rule out the latter because the phosphorescence intensity ratio (I_{ppy}/I_{btp}) was not restored to that of apo form as the temperature was lowered (SI, Figure S6). An average phosphorescence lifetime (τ_{avg}) of the 648 nm decay trace was calculated by using $\tau_{avg} = \Sigma\alpha_i\tau_i^2/\alpha_i\tau_i$ (i = 1−3)[41] with preexponential coefficients (α_i) and time constants (τ_i) obtained with a triple-exponential decay model, giving 4.16 ± 0.21 and 2.47 ± 0.41 μs for the apo and the copper-complexed forms of ZIr2, respectively.

A phosphorescence Job's plot revealed a 1:2 stoichiometry for $CuCl_2$ and the DPA receptor[42−44] of ZIr2 (SI, Figure S7). X-band CW EPR studies of $CuCl_2$ solutions containing various amounts of ZIr2 further confirmed this stoichiometry of copper(II) complexation (SI, Figure S8). In addition, the phosphorescence spectrum of a reference Ir(III) complex lacking a DPA arm showed no copper dependence, indicating that the observed phosphorescence changes are due to DPA−copper ion binding (SI, Figure S9). A binding titration isotherm plotting the phosphorescence intensity ratio (I_{ppy}/I_{btp}) against increasing concentrations of $CuCl_2$ (Figure 2a) was fit to a theoretical model based on

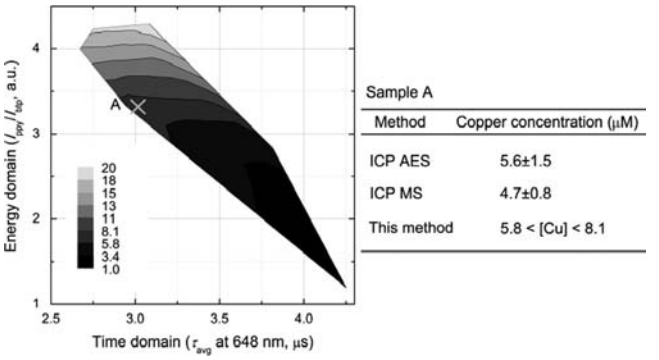

Figure 3. Contour map showing copper concentration as a function of phosphorescence intensity ratio (I_{ppy}/I_{btp}) and average phosphorescence lifetime (τ_{avg}) of ZIr2. Also depicted is the quantitation of copper in sample A using the phosphorescence signals. At the right is a comparison of values determined by ICP-AES, ICP-MS, and the present method.

the calculated concentration of free copper(II) ion, which returned a K_d value of 16 μM (refer to SI for details). Similarly, τ_{avg} decreased with increasing $CuCl_2$ concentrations, leveling off at 1:2 binding (Figure 2a). This result is consistent with the Job's plot and X-band CW EPR titration measurements.

The copper(II) binding and resultant change in phosphorescence intensity ratio and τ_{avg} are reversible. The phosphorescence spectrum of the apo form of ZIr2 was restored by the addition of 100 equiv of Na_2EDTA to a 1:1 mixture of $CuCl_2$ and ZIr2 (Figure 2b). The decay trace at 648 nm displayed similar reversibility (Figure 2c). The invariance of the phosphorescence intensity ratio and τ_{avg} at varying concentrations of ZIr2 and its copper complex in solution or as a suspension (pH 7.0 PIPES buffer containing <2 vol % DMSO; SI, Figures S10 and S11) confirms the robustness of the dual signals. In addition, pH titrations of solutions of ZIr2 and its copper complex reveal the independence of the phosphorescence intensity ratio and τ_{avg} over the pH range 4.5−9.5 (SI, Figures S12 and S13). ZIr2 exhibits excellent selectivity for copper(II) ion over biologically abundant Na^+, K^+, Mg^{2+}, and Ca^{2+} ions, as well as other biologically important transition metal ions, such as divalent Cr, Mn, Fe, Co, Ni, and Zn (Figure 2d).

From the dual-mode signal outputs, we constructed a contour map by which one can quantitate copper(II) ion using our sensor (Figure 3). A notable feature of the map is the availability of two readouts from a single sensor (I_{ppy}/I_{btp} and τ_{avg}), each of which independently reports on the copper concentration. The copper limit of detection (LOD) of the phosphorescence intensity ratio and the average phosphorescence lifetime were calculated to be as low as 35 and 93 ppb, respectively (SI, Figure S14). These values are below national primary drinking water regulation for copper (1.3 ppm) set by U.S. EPA.[45] We therefore employed ZIr2 to investigate real water samples in order to validate its ability to quantify copper concentrations. To water samples collected in Incheon, Korea (SI), we added ZIr2 (10 μM). The phosphorescence intensity ratio and lifetime of the sample were determined to be 3.3 and 3.0 μs, respectively (SI, Figure S15). These values correspond to a copper(II) concentration between 5.8 and 8.1 μM, as shown in Figure 3. The accuracy of this measurement was validated by comparison to values obtained by conventional methods employing ICP-AES (5.6 ± 1.5 μM) and ICP-MS (4.7 ± 0.8 μM).

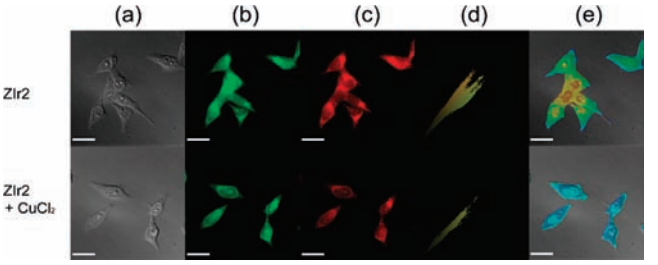

Figure 4. Intracellular copper imaging of fixed HeLa cells treated with 10 μM ZIr2. Cells in the lower panels were incubated with 500 μM $CuCl_2$ prior to ZIr2 treatment. (a) Differential interference contrast images. (b) Phosphorescence acquired through a green channel (excitation band path = 300−390 nm, emission band path = 510−560 nm). (c) Phosphorescence acquired through a red channel (excitation band path = 400−450 nm, emission cut-on for >600 nm). (d) Co-localization scatter plot of green and red channels. (e) Phosphorescence intensity ratio images of green and red channels. Scale bar corresponds to 25 μm, and an identical scale for color mapping was applied to images (e). See Figure S16 in SI for an enlarged version.

As a final demonstration of its applicability to real problems, we studied the ability of our new sensor to detect copper(II) ion exogenously introduced into HeLa cells. An MTT assay revealed that ZIr2 is moderately cytotoxic to HeLa cells (IC_{50} = 42 μM following incubation for 12 h at 37 °C; SI, Figure S17). Nevertheless, ZIr2 could image intracellular copper(II) ions through the generation of ratiometric phosphorescence signals. HeLa cells were incubated either in the presence or in the absence of $CuCl_2$ (500 μM, 2 h)[46] and then thoroughly washed to remove extraneous $CuCl_2$ and detached cells. The cell morphology was carefully examined to ensure that only live cells were subjected to imaging. Healthy cells were then fixed with MeOH and treated with ZIr2 (10 μM in PBS, 0.5 h). Finally, the cells were rinsed repeatedly with fresh PBS. Phosphorescence images were obtained through both green (510−560 nm) and red (>600 nm) channels. As shown in Figure 4b,c, the extracellular region was not luminescent, indicating limited leakage of the sensor and its copper complex during the time scale of our imaging experiment (<15 min). Copper(II) treatment selectively quenched the red channel intensity of HeLa cells, while the green channel images remained relatively intact. Corresponding phosphorescence ratiometric images, as revealed in Figure 4e, were generated by calculating 2D matrix data representing intensity ratios of the green and red images (SI). Co-localization scatter plots for green and red images are diagonal (Figures 4d), which unambiguously indicates that the green and red phosphorescence signals originate from identical positions for both control and copper(II)-treated HeLa cells. The only shortcoming of ZIr2 for biological applications is its limited compatibility with live cells. Nonetheless, ZIr2 should be useful for other tasks, such as quantification of copper in postmortem specimens.

To summarize, we synthesized and characterized ZIr2, the first phosphorescent sensor for quantitating copper(II) ion. The dual-emissive platform based on a multichromophoric iridium(III) complex was successfully implemented to afford a multimodal phosphorescence change upon interaction with copper(II). The sensor operates nicely in pH 7.0 PIPES buffer and exhibits excellent reversibility and selectivity for copper(II) ion, with K_d = 16 μM. Its dual modality, comprising phosphorescence intensity ratio and phosphorescence lifetime readouts, affords robust quantification of copper ion in aqueous media. Intracellular copper ion

imaging was also achieved by using the ratio of phosphorescence signals acquired through green and red channels. The key advantage of ZIr2 is its unique photophysical design that allows the distinct dual emission. In addition, its long luminescence lifetime should enhance the quality of microscopic signals by application of time-gated acquisition.[47] We anticipate that ZIr2 will be a valuable sensor to quantify copper in a range of media.

■ ASSOCIATED CONTENT

Supporting Information. Complete ref 43; experimental details and spectroscopic identification of compounds; Figures S1−S17, displaying the solution UV−vis and phosphorescence spectral behavior of ZIr2 and its Cu^{2+} complex, a Job's plot for ZIr2 complexation with Cu^{2+}, X-band CW EPR spectra of $CuCl_2$ solutions with varying amounts of ZIr2, pH titration of the phosphorescence intensity ratio and lifetime of ZIr2 and its copper complex, determination of the limit of detection of phosphorescence intensity ratio and phosphorescence lifetime, phosphorescence signals of sample A, an enlarged version of Figure 4, and viability data of HeLa cells treated with ZIr2; and Table S1, summarizing TD-DFT results for the reference compound. This material is available free of charge via the Internet at http://pubs.acs.org.

■ AUTHOR INFORMATION

Corresponding Author

odds2@mit.edu (Y.Y.); wwnam@ewha.ac.kr (W.N.); lippard@mit.edu (S.J.L.)

■ ACKNOWLEDGMENT

This work was supported by a grant from the National Institute of General Medical Sciences (Grant GM065519 to S.J.L.). Spectroscopic instrumentation at the MIT DCIF is maintained with funding from NIH Grant 1S10RR13886-01. The research at EWU was supported by NRF/MEST of Korea through the CRI, GRL (2010-00353), and WCU (R31-2008-000-10010-0). Y.Y. acknowledges RP-Grant 2009 of Ewha Womans University. Laser experiments at SNU were supported by CRI Program (RIAMI-AM0209 (0417-20090011)).

■ REFERENCES

(1) Boal, A. K.; Rosenzweig, A. C. *Chem. Rev.* **2009**, *109*, 4760–4779.
(2) Davis, A. V.; O'Halloran, T. V. *Nat. Chem. Biol.* **2008**, *4*, 148–151.
(3) Kim, B.-E.; Nevitt, T.; Thiele, D. J. *Nat. Chem. Biol.* **2008**, *4*, 176–185.
(4) Bergonzi, R.; Fabbrizzi, L.; Licchelli, M.; Mangano, C. *Coord. Chem. Rev.* **1998**, *170*, 31–46.
(5) Shao, N.; Jin, J. Y.; Wang, H.; Zhang, Y.; Yang, R. H.; Chan, W. H. *Anal. Chem.* **2008**, *80*, 3466–3475.
(6) Xiang, Y.; Tong, A.; Jin, P.; Ju, Y. *Org. Lett.* **2006**, *8*, 2863–2866.
(7) Dujols, V.; Ford, F.; Czarnik, A. W. *J. Am. Chem. Soc.* **1997**, *119*, 7386–7387.
(8) Wen, Z.-C.; Yang, R.; He, H.; Jiang, Y.-B. *Chem. Commun.* **2006**, 106–108.
(9) Li, G.-K.; Xu, Z.-X.; Chen, C.-F.; Huang, Z.-T. *Chem. Commun.* **2008**, 1774–1776.
(10) Jung, H. S.; Park, M.; Han, D. Y.; Kim, E.; Lee, C.; Ham, S.; Kim, J. S. *Org. Lett.* **2009**, *11*, 3378–3381.
(11) Kim, H. J.; Hong, J.; Hong, A.; Ham, S.; Lee, J. H.; Kim, J. S. *Org. Lett.* **2008**, *10*, 1963–1966.
(12) Ciesienski, K. L.; Hyman, L. M.; Derisavifard, S.; Franz, K. J. *Inorg. Chem.* **2010**, *49*, 6808–6810.
(13) Wu, Q.; Anslyn, E. V. *J. Am. Chem. Soc.* **2004**, *126*, 14682–14683.
(14) Demchenko, A. P. *FEBS Lett.* **2006**, *580*, 2951–2957.
(15) Vinkenborg, J. L.; Koay, M. S.; Merkx, M. *Curr. Opin. Chem. Biol.* **2010**, *14*, 231–237.
(16) Chang, C. J.; Jaworski, J.; Nolan, E. M.; Sheng, M.; Lippard, S. J. *Proc. Natl. Acad. Sci. U.S.A.* **2004**, *101*, 1129–1134.
(17) Zhou, Y.; Wang, F.; Kim, Y.; Kim, S.-J.; Yoon, J. *Org. Lett.* **2009**, *11*, 4442–4445.
(18) Royzen, M.; Dai, Z.; Canary, J. W. *J. Am. Chem. Soc.* **2005**, *127*, 1612–1613.
(19) Xu, Z.; Xiao, Y.; Qian, X.; Cui, J.; Cui, D. *Org. Lett.* **2005**, *7*, 889–892.
(20) Kasha, M. *Faraday Soc. Discuss.* **1950**, *9*, 14–19.
(21) Song, L.-q.; Feng, J.; Wang, X.-s.; Yu, J.-h.; Hou, Y.-j.; Xie, P.-h.; Zhang, B.-w.; Xiang, J.-f.; Ai, X.-c.; Zhang, J.-p. *Inorg. Chem.* **2003**, *42*, 3393–3395.
(22) Spencer, B. R.; Kraft, B. J.; Hughes, C. G.; Pink, M.; Zaleski, J. M. *Inorg. Chem.* **2010**, *49*, 11333–11345.
(23) Glazer, E. C.; Magde, D.; Tor, Y. *J. Am. Chem. Soc.* **2005**, *127*, 4190–4192.
(24) Glazer, E. C.; Magde, D.; Tor, Y. *J. Am. Chem. Soc.* **2007**, *129*, 8544–8551.
(25) Nahhas, A. E.; Consani, C.; Blanco-Rodríguez, A. M.; Lancaster, K. M.; Braem, O.; Cannizzo, A.; Towrie, M.; Clark, I. P.; Záliš, S.; Chergui, M.; Vlček, A., Jr. *Inorg. Chem.* **2011**, *50*, 2932–2943.
(26) Wallace, L.; Jackman, D. C.; Rillema, D. P.; Merkert, J. W. *Inorg. Chem.* **1995**, *34*, 5210–5214.
(27) Wallace, L.; Rillema, D. P. *Inorg. Chem.* **1993**, *32*, 3836–3843.
(28) Wallace, L.; Woods, C.; Rillema, D. P. *Inorg. Chem.* **1995**, *34*, 2875–2882.
(29) You, Y.; Seo, J.; Kim, S. H.; Kim, K. S.; Ahn, T. K.; Kim, D.; Park, S. Y. *Inorg. Chem.* **2008**, *47*, 1476–1487.
(30) You, Y.; Park, S. Y. *J. Am. Chem. Soc.* **2005**, *127*, 12438–12439.
(31) You, Y.; Kim, K. S.; Ahn, T. K.; Kim, D.; Park, S. Y. *J. Phys. Chem. C* **2007**, *111*, 4052–4060.
(32) Lo, K. K.-W.; Zhang, K. Y.; Leung, S.-K.; Tang, M.-C. *Angew. Chem., Int. Ed.* **2008**, *47*, 2213–2216.
(33) Park, G. Y.; Kim, Y. S.; Ha, Y. *Curr. Appl. Phys.* **2007**, *7*, 390–395.
(34) Zhao, Q.; Huang, C.; Li, F. *Chem. Soc. Rev.* **2011**, *40*, 2508–2524.
(35) Lo, K. K.-W.; Li, S. P.-Y.; Zhang, K. Y. *New J. Chem.* **2011**, *35*, 265–287.
(36) Zhao, Q.; Li, F.; Huang, C. *Chem. Soc. Rev.* **2010**, *29*, 3007–3030.
(37) Chi, Y.; Chou, P.-T. *Chem. Soc. Rev.* **2010**, *39*, 638–655.
(38) Erickson, K.; Braun, R. D.; Yu, D.; Lanzen, J.; Wilson, D.; Brizel, D. M.; Secomb, T. W.; Biaglow, J. E.; Dewhirst, M. W. *Cancer Res.* **2003**, *63*, 4705–4712.
(39) Berezin, M. Y.; Achilefu, S. *Chem. Rev.* **2010**, *110*, 2641–2684.
(40) Chao, S.-h.; Holl, M. R.; McQuaide, S. C.; Ren, T. T. H.; Gales, S. A.; Meldrum, D. R. *Opt. Express* **2007**, *15*, 10681–10689.
(41) Ruedas-Rama, M. J.; Orte, A.; Hall, E. A. H.; Alvarez-Pez, J. M.; Talavera, E. M. *Chem. Commun.* **2011**, *47*, 2898–2900.
(42) Turba, S.; Walter, O.; Schindler, S.; Nielsen, L. P.; Hazell, A.; McKenzie, C. J.; Lloret, F.; Cano, J.; Julve, M. *Inorg. Chem.* **2008**, *47*, 9612–9623.
(43) Antonioli, B.; et al. *Dalton Trans.* **2009**, 4795–4805.
(44) Blindauer, C. A.; Razi, M. T.; Parsons, S.; Sadler, P. J. *Polyhedron* **2006**, *25*, 513–520.
(45) U.S. EPA. EPA 816-F-09-0004, May 2009.
(46) This incubation condition seems to be cytotoxic to HeLa cells, but there are reports where harsher copper incubation conditions have been employed for fluorescent copper imaging: (a) Domaille, D. W.; Zeng, L.; Chang, C. J. *J. Am. Chem. Soc.* **2010**, *132*, 1194–1195. (b) Jiao, L.; Li, J.; Zhang, S.; Wei, C.; Hao, E.; Vicente, M. G. H. *New J. Chem.* **2009**, *33*, 1888–1893. (c) Yu, M.; Shi, M.; Chen, Z.; Li, F.; Li, X.; Gao, Y.; Xu, J.; Yang, H.; Zhou, Z.; Yi, T.; Huang, C. *Chem. Eur. J.* **2008**, *14*, 6892–6900.
(47) You, Y.; Park, S. Y. *Adv. Mater.* **2008**, *20*, 3820–3826.